Research Square

Preprints are preliminary reports that have not undergone peer review.
They should not be considered conclusive, used to inform clinical practice,
or referenced by the media as validated information.

Enhanced modeling of expandable polystyrene synthesis: effects of n-pentane on polymerization process dynamics

Jeorge Luís dos Santos Amaral
Rodrigo Battisti
rodrigo.battisti@ifsc.edu.br

Federal Institute of Education Science and Technology of Santa Catarina: Instituto Federal de Educacao Ciencia e Tecnologia de Santa Catarina https://orcid.org/0000-0002-7763-4015

Ricardo Antonio Francisco Machado
Cintia Marangoni

Research Article

Keywords: Expandable polystyrene, Suspension polymerization, Blowing agent, User-model routines, Aspen Polymers

Posted Date: November 20th, 2026

DOI: https://doi.org/10.21203/rs.3.rs-11636934/v1

License: This work is licensed under a Creative Commons Attribution 4.0 International License.
Read Full License

Enhanced modeling of expandable polystyrene synthesis: effects of *n*-pentane on polymerization process dynamics

Jeorge Luís dos Santos Amaral [1], Rodrigo Battisti [2*], Ricardo Antonio Francisco Machado [1], Cintia Marangoni [1]

[1] *Chemical Engineering Graduate Program, Federal University of Santa Catarina, Trindade campus, 88040-900, Florianópolis, Brazil*

[2] *Federal Institute of Education, Science and Technology of Santa Catarina, Criciúma campus, 88813-600, Criciúma, Brazil*

Corresponding Author: Prof. Rodrigo Battisti. *****E-mail: rodrigo.battisti@ifsc.edu.br

ABSTRACT: Expandable polystyrene (EPS) polymerization and impregnation processes were performed in Aspen Polymers software with modifications implemented through innovative user-model routines in order to represent the effect of the blowing agent (*n*-pentane) on the process dynamics. The modified model showed errors below 10% compared to experimental data from the literature, validating the process. Then, four EPS synthesis scenarios were proposed to improve batch cycles. The application of heating ramp and intermediate dosage of initiator – after 70% of conversion – was efficient for a high conversion production of EPS with more homogeneous properties, which guarantees a commercial-grade product without residual monomer. The continuous dosage of the blowing agent since the beginning of the polymerization was effective in minimizing the gel and glassy effects, besides eliminating the *n*-pentane addition step and reducing the batch cycle. Therefore, the commercial simulation model modified with the novel user-model routines implemented proved to be effective in improving the dynamics of the EPS synthesis process.

Keywords: Expandable polystyrene · Suspension polymerization · Blowing agent · User-model routines · Aspen Polymers.

1 Introduction

Expandable polystyrene (EPS) is a versatile thermoplastic used worldwide in foamed materials such as disposable serving trays, cups, packaging materials, containers, and insulation boards for floors, walls, and roofs in buildings [1–3]. The most often large-scale method used to produce expandable polystyrene beads is the suspension polymerization with a blowing agent (often a volatile hydrocarbon) incorporated in the polymer beads. This process consists of two steps, namely the polymerization in aqueous suspension where the beads are formed, followed by the impregnation with the addition of a blowing agent, which diffuses into the particles [4]. The blowing agent vaporizes when the beads are heated with steam, then beads expand and fuse to form a semi-rigid foam [5]. The polymerization of polystyrene is performed at around 90 °C to 125 ºC. It is carried out in batch reactors with volumetric fractions of the dispersed phase (styrene) in the range of 0.4 to 0.6, so-called holdup until conversions in which the spheres become glassy due to the glass transition temperature of the monomer/polymer mixture [6]. The impregnation stage is conducted at higher temperatures and pressures with the blowing agent, commonly the *n*-pentane or a mixture of *n*-pentane and iso-pentane, being fed to the reactor to diffuse through the spheres. Some processes impregnate with butane, but it is not commonly used today [1, 2]. Depending on the temperature and pressure of impregnation, a minimum time must be allowed for the diffusion of the blowing agent to reach the core of the beads [7, 8].

Great advances in styrene suspension polymerization were triggered by simulated studies towards kinetic modeling, new reactor designs, and specific configurations. Machado et al. [9] proposed a population balance model with experimental validation for the production of polystyrene via suspension polymerization, describing with good accuracy the evolution of particle size distribution of the polymer matrix. Curteanu [10] investigated the modeling and simulation of styrene polymerization via free radicals in a semi-batch reactor. The author indicated the intermediate addition of an initiator as a method for controlling the polymer

properties. Almeida et al. [11] developed a model for predicting the steady-state and dynamic behavior of a continuous styrene polymerization process. The main parameters were estimated from the data of an industrial plant. To study the physical properties of polystyrene, Srivastava and Ghosh [12] developed a molecular dynamic model in order to assess the polystyrene glass transition temperature. Vieira and Lona [13] used a kinetic modeling to analyze the effect of temperature on the polystyrene properties obtained by radical polymerization by atom transfer, providing a tool for process optimization. More recently, Khajehpour-Tadavani et al. [14] developed a modified Monte Carlo model to predict particle size distributions during PS and EPS suspension polymerization, accounting for the effects of suspending agents, reactor configurations, operating conditions, and pentane addition. The model showed good agreement with experimental data, highlighting its applicability to predicting particle size evolution under different polymerization conditions. Although bulk polymerization of styrene in plug flow reactors has been well and successfully reported [15], recent literature showed alternatives for implementing suspension polymerization via continuous reactor, a process traditionally carried out in batch reactors, thus providing technical and economic advantages [16].

Despite the advances regarding suspension polymerization, there are few studies that specifically deal with the impregnation of the polymer matrix using a blowing agent. Still, these few existing works seldom investigate the parameters concerning the final product's properties in the blowing agent's presence. Salejova and Kosek [17] found that the amount of *n*-pentane sorbed in polystyrene particles and the impregnation time directly influence the morphology of the arisen foam. Short impregnation time leads to the formation of small individual cells and homogeneous cellular structure of the expanded particle. During long impregnation time, the final cellular structure of the expanded particle becomes heterogeneous, and large semi-transparent bubbles randomly arise close to the particle surface. The vast majority of the works dealing with polystyrene impregnation are experimental. However, simulation is of paramount

importance in the polymerization process field, being low-cost support in decision making and the development new production routes [11]. Victoria-Valenzuela and Morales-Cepeda [18] investigated the influence of *n*-pentane on the kinetics of bulk styrene polymerization through mathematical modeling. Their results highlighted the importance of diffusion-controlled termination, solvation, and chain-transfer effects in describing polymerization behavior and predicting the evolution of weight-average molecular weight. The investigation of polymerization processes using commercial simulators has recently gained prominence. Lesage et al. [19] identified kinetic reaction parameters in the Aspen Custom Modeler with dynamic simulations of a CSTR for the propylene gas polymerization. Funai et al. [20] used Aspen Polymers to validate a model of the hydrolytic polymerization process of Nylon in a laboratory-scale semi-stacked reactor. Kusolsongtawee and Bumroongsri [21] presented a model of a fluidized bed polymerization reactor applied in the production of low-density polyethylene using the Aspen Custom Modeler software to obtain specific polymer characteristics and investigate the flow behavior in the reactor.

Achieving improvements in the polymerization processes is constantly demanded. In this sense, the manipulation of process variables and parameters is an economical alternative for improving such polymerization systems, bringing considerable reductions in batch cycles without changes to the properties of the produced polymer [22]. In this context, the present work aims to evaluate alternative production routes of styrene polymerization using the commercial software Aspen Polymers to boost process productivity. For this purpose, the standard model of Aspen Polymers software was modified with innovative user-model routines to consider the effect of the blowing agent in the polymerization process. After the simulation validated by experimental data from the literature, the application of heating ramps and different dosages of initiator and blowing agent in EPS production was investigated. Improved routes were achieved by

accessing quickly and economically conversion data, weight-average molar masses, and molar mass distribution at the end of the batch reaction.

2 Methodology

2.1 Reaction mechanism

The set of elementary reactions involved in the mechanism of the suspension polymerization of styrene with a monofunctional initiator considered in this study includes, as showed in Eq. (1) to Eq. (5): (1) chemical initiation stage; (2) chain initiation; (3) propagation reaction; (4) chain transfer or inhibition reaction; and at least one (5) termination step to produce the dead polymer, as these reactions occur simultaneously during polymerization [23, 24]. Free radical suspension polymerizations follow the same kinetic mechanism throughout the reaction [25]. For styrene, thermal initiation can be neglected in reactions conducted below 100 °C, and termination by combination is predominant in the polymerization of styrene [23, 25].

$$I \xrightarrow{k_\mathrm{d}} 2 \cdot R \tag{1}$$

$$R + M \xrightarrow{k_\mathrm{i}} P_1 \tag{2}$$

$$P_\mathrm{n} + M \xrightarrow{k_\mathrm{p}} P_{\mathrm{n}+1} \tag{3}$$

$$P_\mathrm{n} + M \xrightarrow{k_\mathrm{tf}} D_\mathrm{n} + P_1 \tag{4}$$

$$P_\mathrm{n} + P_\mathrm{m} \xrightarrow{k_\mathrm{tc}} D_{\mathrm{n}+\mathrm{m}} \tag{5}$$

In all equations, I is the monofunctional initiator, M is the styrene monomer, R is the primary radical. P_n and D_n represent, respectively, the living and dead polymer molecules of chain length n. However, not all radicals start a chain, so an efficiency factor f is usually associated with the initiator's efficiency [26]. The physical and mechanical properties of the polymer are related to the numerical average molar masses, as showed by Eq. (6), and weight average molar

masses by Eq. (7), which in turn are related to the moments of the polymer distributions. MM_m is the molar mass of the monomer.

$$M_{\mathrm{n}} = MM_{\mathrm{m}}.\frac{\mu_1 + \lambda_1}{\mu_0 + \lambda_0} \tag{6}$$

$$M_{\mathrm{w}} = MM_{\mathrm{m}}.\frac{\mu_2 + \lambda_2}{\mu_1 + \lambda_1} \tag{7}$$

The k^{th} moment of living polymers is defined as:

$$\lambda_{\mathrm{k}} = \sum_{n=0}^{\infty} n^k.[P_{\mathrm{n}}] \tag{8}$$

The k^{th} moment of the dead chains is defined as:

$$\mu_{\mathrm{k}} = \sum_{n=0}^{\infty} n^{\mathrm{k}}.[D_{\mathrm{n}}] \tag{9}$$

2.2 Simulation design

The suspension polymerization process of styrene was modeled in the Aspen Polymers software using the batch reactor unit. The reactants adopted were benzoyl peroxide (BPO, initiator), styrene (dispersed phase, monomer), water (continuous phase), and *n*-pentane (blowing agent). The polymerization reactions occur in the organic liquid phase (drops of monomer/polymer) [27]. The polymerization reactions expressed in Eq. (1) to Eq. (5) were specified to compose the simulated reaction mechanism. The parameters required for calculating the reaction rate constants, the pre-exponential factors, and the activation energies are shown in Table 1. It is important to highlight that the parameters used for the chain initiation step are the same as the propagation step, as the chemical nature of both reactions is the same. For predicting physical properties, the thermodynamic model of the liquid activity coefficient

of a polymeric system (POLYNRTL) was used. The physicochemical properties of the polymer were calculated using Van Krevelen's group contribution method [28].

Table 1 Parameters for reaction rate calculation

Reaction step	Pre-exponential factor (h^{-1})	Activation energy ($kcal \cdot mol^{-1}$)	Reference
Initiation	1.38×10^{16}	27.2	Villalobos et al. [29]
Thermal initiation	7.89×10^{8}	27.4	Choi et al. [30]
Propagation	3.68×10^{10}	7.10	Mahabadi and O'Driscoll [31]
Termination	4.53×10^{12}	1.68	Mahabadi and O'Driscoll [31]
Chain transfer	3.68×10^{10}	13.45	Mahabadi and O'Driscoll [31]

2.2.1 Modifications implemented to address the gel and glassy effects

The standard gel effect correlations of Aspen Polymers are empirical models adjusted from experimental data. These refer only to the gel effect in polymerization reactions without impregnation and do not represent the glass effect. However, *n*-pentane (nP_5) is the EPS solvent and rubberizes the polymer matrix. It is known that adding a solvent to the system alters the global free volume. This alteration directly influences the polymerization kinetics leading to different behaviors regarding the gel and glass effects [24]. Therefore, in the present work, the correlations expressed in Eq. (10) and Eq. (11) were incorporated in Aspen Polymers through user-model routines written in a programming language based on the free volume theory. Using these user-model correlations leads to simulations capturing the influence of the impregnating agent on the polymeric matrix. Eq. (10) was specified to modify the termination rate constant (k_{tc}) due to the gel effect, while Eq. (11) was used to adjust the propagation rate constant (k_p) due to the glass effect.

$$k_{\mathrm{tc}}(X) = k_{\mathrm{tc0}} \cdot \left(1 + \delta \cdot [P](X)\right) \cdot \left(\frac{M_{\mathrm{wcr}}}{M_{\mathrm{w}}(X)}\right)^{N} \cdot exp\left[-A \cdot \left(\frac{1}{VF(X)} - \frac{1}{VF_{\mathrm{cr1}}}\right)\right] \tag{10}$$

$$k_{\mathrm{p}}(X) = k_{\mathrm{p0}} \cdot exp\left[-B \cdot \left(\frac{1}{VF(X)} - \frac{1}{VF_{\mathrm{cr2}}}\right)\right] \tag{11}$$

Where $VF_{\mathrm{i}}(X)$, defined as the free volume of species *i* in the reaction, is calculated by Eq. (12), and VF_{cr1} is calculated by the same equation in the conversion where the termination reaction becomes controlled by translational diffusion.

$$VF_{\mathrm{i}}(X) = \left[0.025 + \alpha_{\mathrm{i}} \cdot \left(T - T_{\mathrm{gi}}\right)\right] \cdot \left(\frac{V_{\mathrm{i}}(X)}{V(X)}\right) \tag{12}$$

where α_{i} is the thermal expansion coefficient of species *i*, and T_{gi} is the glass transition temperature of species *i*. The free volume of the system at any conversion is then given by:

$$VF(X) = VF_{\mathrm{m}}(X) + VF_{\mathrm{p}}(X) \quad \text{for } X < X_{\mathrm{s}} \tag{13}$$

Or

$$VF(X) = VF_{\mathrm{m}}(X) + VF_{\mathrm{p}}(X) + VF_{\mathrm{s}} \quad \text{for } X \geq X_{\mathrm{s}} \tag{14}$$

2.3 Experimental validation

Experimental validation is essential to ensure the reliability and predictive accuracy of mathematical models implemented in commercial simulation software [32]. Comparing simulated results with experimental data allows the assessment of model deviations and its ability to reproduce actual process behavior, providing a reliable basis for evaluating alternative operating conditions and optimizing polymerization processes. To validate the mathematical

model and all modifications proposed in the simulator, part of the work presented by Villalobos et al. [24] was replicated. The authors studied the effect of adding the impregnating agent in several reaction stages. Suspension polymerization and impregnation of polystyrene with *n*-pentane were carried out in a 3.2 L reactor with a Rushton stirrer-type at 350 rpm, 90 °C, and an initiator concentration (BPO) of 0.01 $mol \cdot L^{-1}$ of styrene. The suspending agent was tricalcium phosphate (TCP) at a concentration of 7.5 $g \cdot L^{-1}$. Three situations were studied, with no adding *n*-pentane (standard, 0 wt% *n*-P_5), 7.5% *n*-pentane (7.5 wt% *n*-P_5), and 15% *n*-pentane (15 wt% *n*-P_5), with the blowing agent being added to the system from the beginning of the reactions. To demonstrate the specific improvements obtained with the modified model with user-model correlations, the simulation with 7.5% *n*-P_5 was performed in 3 configurations: (i) without the gel-effect correlations; (ii) using the standard gel-effect correlations from the commercial software; (iii) using the novel user-model correlations implemented in the commercial software. The three situations were compared with the experimental data to consolidate the best simulation model.

2.4 Proposed scenarios

Four scenarios were proposed for expandable polystyrene production from the best model previously validated. In these scenarios, the effects on the polymerization kinetics and final characteristics of the polymer caused by the manipulation of process variables were evaluated. The application's versatility in calculating reaction and product properties, such as weighted-average molar mass (M_w) distribution, polydispersity index (PDI), and final monomer conversion, was explored since these properties provide important information about the characteristics of the produced polymer. Table 2 shows the manipulated variables and the operational conditions used in the four proposed scenarios.

Table 2 Operational conditions and formulations of the proposed scenarios

Scenario	Type of reactor	BPO	*n*-Pentane	Temperature
1	Batch	0.01 mol·L^{-1}	0% (standard); 7.5%; 15%	0.54 °C·min^{-1}
2	Semi-batch	0.1 mol·min^{-1} 0.2 mol·min^{-1} 0.4 mol·min^{-1}	0% (standard)	90 °C (isothermal)
3	Semi-batch	0.01 mol·L^{-1}	0.005 kg·h^{-1} (7.5% at end of reaction)	90 °C (isothermal)
4	Semi-batch	0.01 mol·L^{-1} [(a)] 0.1 mol·min^{-1} [(b)]	0.005 kg·h^{-1} (7.5% at end of reaction)	90 °C [(a)] 0.5 °C·min^{-1} [(b)]

[(a)] at the beginning of the reaction (0 min)

[(b)] 360 to 420 min of the reaction

2.4.1 Scenario 1

The usual route for polystyrene production begins with the formulation loading in the reactor without the initiator. Then heating is carried out to the reaction temperature – normally 90 °C – and the initiator is added to start the polymerization [33]. Although this route is classic and functional, there are two main disadvantages: (i) long preparation and heating time, which is a non-productive period, as there is no reaction without the addition of the initiator; (ii) as the reaction only starts at 90 °C the monomer is exposed to high temperatures for a long period, and there is high vaporization, which requires a condensation and monomer recovery system in the polymerization reactors. So, in order to minimize these disadvantages, two modifications to the production route were proposed:

i. Loading the reactor at room temperature with the initiator present in the mixture;

ii. Applying a controlled heating ramp until the desired reaction temperature is reached.

These changes sought to reduce the preparation time and allow the monomer consumption to start as soon as possible, even during the heating ramp, thus leading to higher productivity and shorter batch cycles. Thus, in scenario 1, the application of heating ramps was evaluated, and the non-isothermal behavior of the system can be studied. Due to the viscous effects, temperature control in suspension polymerization reactors is not trivial. Moreover, heating in the presence of the initiator requires high caution since the poor distribution and removal of heat generated by the exothermic reaction can lead to loss of suspension stability and complete loss of reactor load. With this in mind, a soft heating ramp from 25 °C to 90 °C for 120 min was proposed in this scenario. In this way, the reactor was configured as non-isothermal, and a linear heating rate of 0.54 $°C \cdot min^{-1}$ was applied.

2.4.2 Scenario 2

The proposal for scenario 2 was to study the semi-batch reaction with a continuous dosage of initiator to mitigate the effects of the high concentration in the reaction medium. For observing the isolated effect of the continuous dosage of the initiator, a simulation without the addition of *n*-P_5 was built. The suspending agent TCP was added at 7.5 $g \cdot L^{-1}$. In order to investigate the effect of the initiator concentration in the semi-batch process, double and quadruple of the standard value was stipulated. Three BPO dosage rates were simulated: 0.1 $mol \cdot min^{-1}$, 0.2 $mol \cdot min^{-1}$, and 0.4 $mol \cdot min^{-1}$. The molar flow rate of 0.1 $mol \cdot min^{-1}$ corresponds to 0.01 $mol \cdot L^{-1}$ at the end of the dosage.

2.4.3 Scenario 3

In the conventional EPS production route, *n*-P_5 is added to the reactor when the conversion is close to 100% [34]. The blowing agent is dosed in the system for a long period, suitable for the spherical EPS particles to absorb it without becoming sticky. After the temperature has been raised above both the pentane boiling point (36.1 °C) and the pentane-swollen polystyrene glass

transition temperature (97.6 ± 1.0 °C), the polymer beads expand and acquire a cellular microstructure [35]. Once again, thinking about the reduction of long batch cycles, in scenario 3, the dosage of *n*-P_5 was added continuously from the beginning of the reaction until the end. Thus, the semi-batch process was again evaluated, but in this case, with a continuous dosage of *n*-P_5.

2.4.4 Scenario 4

Scenario 4 is an extension of scenario 3 as an alternative leading to conversions higher than 95%. For this, the effect of the temperature rising and the addition of more initiator in the final reaction period was investigated. Performing temperature ramps and BPO dosage in the final reaction periods were studied. From the condition exposed in scenario 3, a heating ramp of 0.5 °C·min^{-1} (from 360 to 420 min) was applied. In addition to the temperature, the dosage of BPO at a rate of 0.1 mol·min^{-1} was added for one hour from 360 to 420 min.

2.5 Treatment of model deviations

To validate the proposed modified model, the mean squared error (MSE) was calculated to measure the agreement between simulated data and experimental values obtained from Villalobos et al. [24], as shown by Eq. (15).

$$\mathrm{MSE} = \frac{1}{n}\sum_{i=1}^{n}\left(Y_\mathrm{i} - \hat{Y}_\mathrm{i}\right)^2 \tag{15}$$

The mean absolute percentage error (MAPE) was also calculated for each evaluated scenario according to Eq. (16), as the average between the errors of the simulated points.

$$\mathrm{MAPE} = \frac{1}{n}\sum_{i=1}^{n}\left(\frac{Y_\mathrm{i} - \hat{Y}_\mathrm{i}}{Y_\mathrm{i}}\right)\cdot 100 \tag{16}$$

3 Results and discussions

3.1 Validation analysis

Figure 1 shows that in the absence of *n*-P_5, the gel effect started at around 50% conversion. The reduction in the conversion rate in the final reaction stages due to the glass effect is also perceived by the curvature. By the graphical analysis, it can be concluded that in the two cases with the presence of *n*-P_5, two main differences were observed concerning the case in the absence of *n*-P_5: first, a slight decrease in the initial conversion rate; and second, there was no occurrence of gel and glass effects. The conversion rate decrease obtained in the simulated data can be explained by the lower concentration of monomer and initiator due to the presence of *n*-P_5, which, consequently, acts as a diluent. The gel effect does not occur because *n*-P_5 has a plasticizing effect that increases the diffusion of the growing polymer chains, which prevents the start of the diffusion-controlled termination. The glass effect also is not observed in the presence of the blowing agent since the T_g of the polystyrene (PS) with 7.5 wt% and 15 wt% of *n*-P_5 is well below 90 °C (T_g^{PS} = 97 °C and T_g^{nP5} = -150 °C).

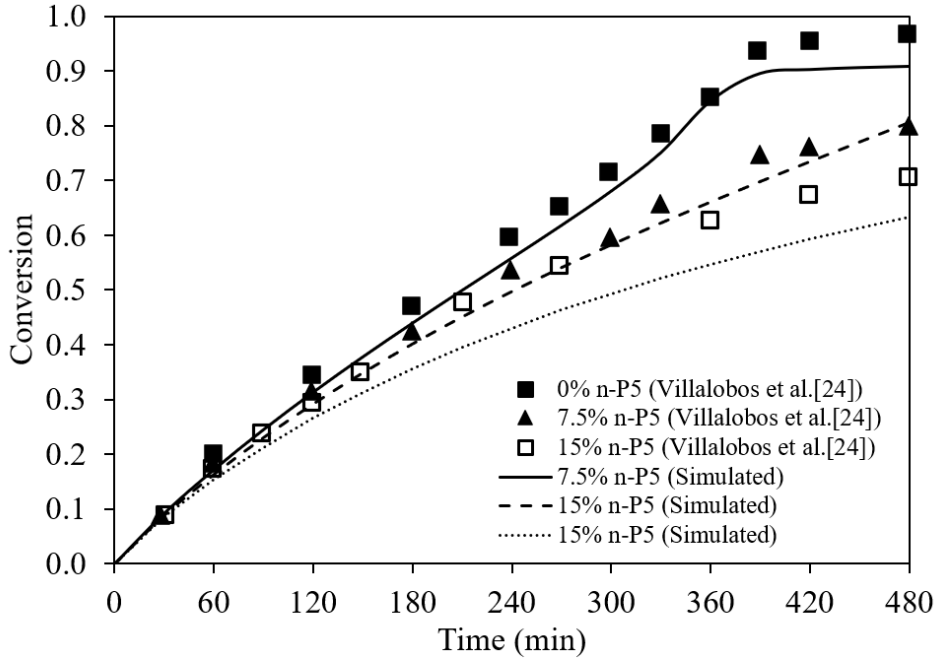


Fig. 1 Comparative conversion profiles considering different concentrations of *n*-P5

As can be seen in Figure 1, the user-model correlations implemented for the gel and glass effects enabled the simulations to reproduce the effects observed experimentally, allowing to quantify the influence of the plasticizer in the reaction medium in all cases. However, the error is higher when the *n*-P_5 content in the process increases (15%). It occurs because in the polymerization processes by free radicals, the phenomena controlled by diffusion occur simultaneously with chemical reactions. Despite taking into account such diffusion processes, the theory of volume becomes less representative in systems where the processes of diffusion predominate [36]. This case refers to the high concentration of the impregnating agent, as its presence intensifies the movement of macromolecules. Table 3 shows the statistical deviation results for each situation reproduced. It is possible to conclude that the best-simulated scenario was in the presence of 7.5 wt% of *n*-P_5, as it has the lowest MSE (1.079×10^{-3}) and MAPE (5.8%). Regarding the selection of mathematical models, Tefera et al. [37] evaluated four models for polymerization via free radicals, and all models showed errors of up to 10% in the simulations used to estimate parameters. Thus, the other cases in the present study were considered acceptable, as they presented MAPE below 10%.

Table 3 Deviations between experimental and simulated data for each conversion

	0% *n*-P_5	**7.5% *n*-P_5**	**15% *n*-P_5**
MSE	0.001419	0.001079	0.001757
MAPE	7.1%	5.8%	7.3%

Figure 2 shows the simulated and experimental points for the weight-average molar mass profile as a function of conversion. It is possible to observe that, qualitatively, the behavior was well adequate. However, the errors obtained are relatively high, close to the acceptable limit (10%). The MAPE values for the standard condition (0% of *n*-P_5) was 8.5%; for the 7.5% *n*-P_5 condition, it was 10.3%, and for the 15% *n*-P_5 condition, it was 8.7%. As shown in Figure 2, the proposed user-model routine for predicting the weight-average molar mass captured the

system's behavior, which justifies its application in the study of EPS production scenarios. For the conversion data and the graphical analysis, the MSE in the order of 10^{-3} and MAPE below 10% assure a substantial qualitative and quantitative agreement between simulated and experimental data. Therefore, the simulation implemented in the Aspen Polymers software is representative, being an effective tool for the study of improvement of the EPS synthesis in the presence or absence of the blowing agent (*n*-P_5) during the styrene polymerization.

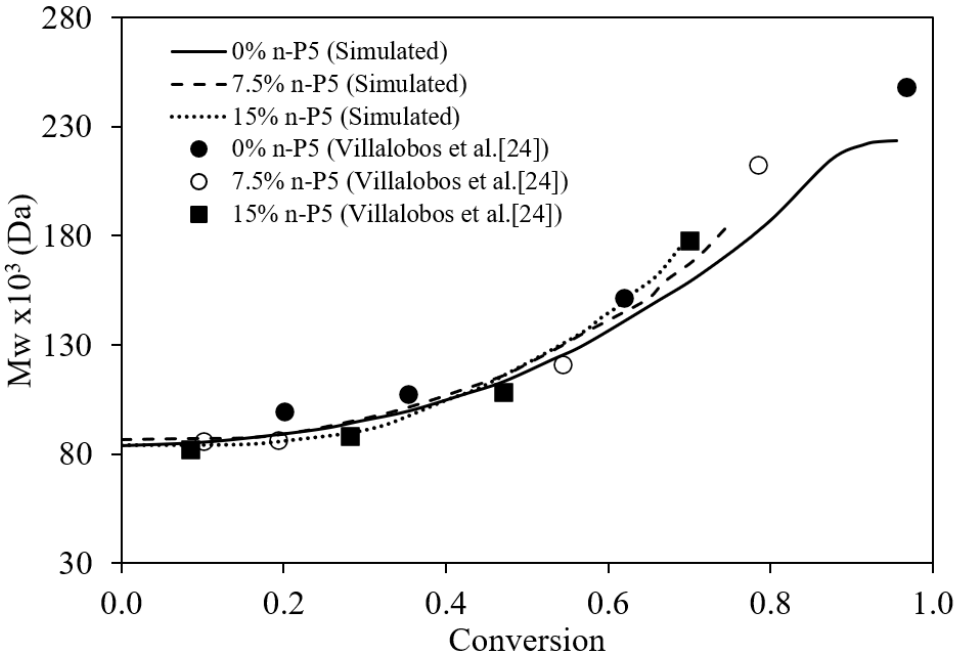


Fig. 2 Evolution of the weight-average molar mass as a function of the conversion

3.2 Scenario 1 evaluation

Figure 3 (a) shows the conversion curves obtained for scenario 1. Similar behavior can be observed in the three cases. The reaction rate in the initial 60 min is around 80% lower when compared to the validation tests. The conversion rate increased 37% after 90 min when the temperature is already above 70 °C. Compared to the cases without temperature ramp used in the validation, the final conversions are very low, reaching less than 40% for the best case. In the first 120 min of the reaction – non-isothermal period – the kinetics are completely different from the isothermal case studied in the validation; this shows the non-isothermal effect on the

conversion dynamics [38]. Even after 120 min – isothermal period – the conversion rate does not reach the levels obtained in the standard simulations. This shows that – even if applied only for a period (120 min) – the temperature ramp influences the entire reaction. As stated by Odian [39], the BPO half-life is only 19.8 min at 100 °C, and when the temperature is reduced by 70 °C, this value rises to 438 min, i.e., with a reduction of only 30 °C, the half-life increases more than 20 times. Thus, the conversion rate was reduced a lot in the first 120 min of reaction since the decomposition of the initiator is extremely slow at temperatures below 90 °C. For these reasons, achieving a reasonable conversion at the end of the reaction time was impossible. Figure 3 (b) shows the evolution of the weight-average molar mass over the conversion for the three cases in scenario 1 (Ramp *T*) compared to the validation cases (Constant *T*). It is observed the formation of polymeric chains of higher molar mass at the beginning of the reaction when the temperature is still low and the chain propagation reactions are favored. However, the weight-average molar masses decrease during the reaction until reaching a minimum. With the temperature increase, there is an increase in the termination rate, and chains of lower average molar mass are formed when compared to the beginning of the reaction. This behavior is completely different from what was observed in the validation simulations with constant temperature. The dynamics of the process was completely different, which led, consequently, to different final products. The results shown in Figure 3 (c) with the data presented in Table 4 relate to the characteristics of the final product. The narrow molar mass distribution curves, the polydispersity values, and the final weight-average molar mass led to conclude that the application of the heating rate allows the synthesis of polystyrene with lower molar mass and more homogeneous. Although the heating ramp is a good expedient for controlling the final properties of polystyrene, a 40% conversion rate is not economically advantageous. In addition to being inefficient, there is no way to unload a reactor with conversion below the PIP (particle identification point) [40]. Thus, the application of this device requires precaution and justifies the manipulation of other process variables that can guarantee better control of the reaction.

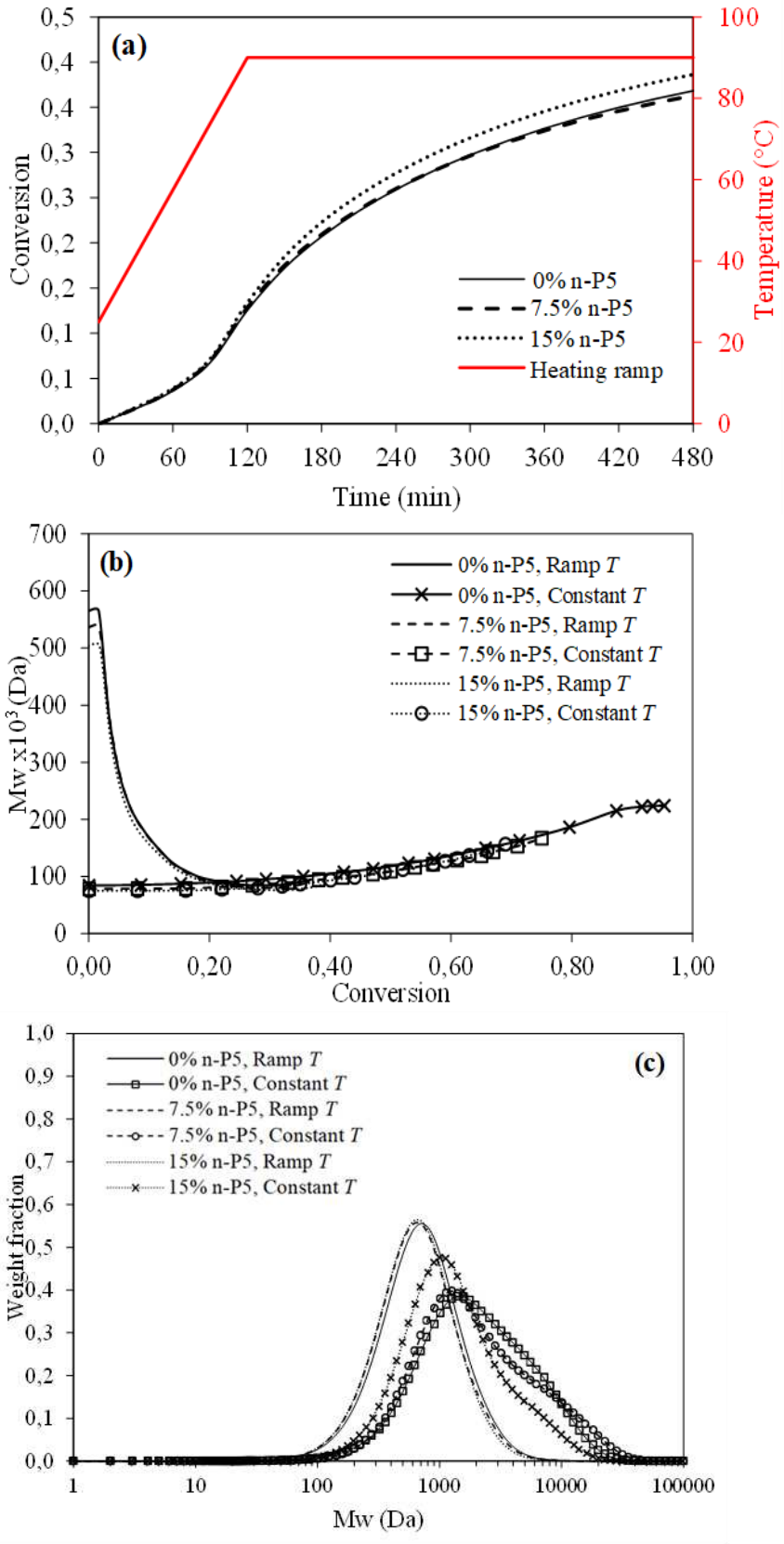


Fig. 3 Scenario 1: (a) conversion profile and reaction temperature; (b) evolution of weight-average molar mass as a function of the conversion; (c) molar mass distribution at the end of the reaction.

Table 4 Polydispersity index (PDI) for reactions conducted in scenario 1

		0% *n*-P5	**7.5% *n*-P5**	**15% *n*-P5**
Constant *T*	PDI	2.83	2.94	2.30
	M_w (Da)	224×10^3	168×10^3	157×10^3
Ramp *T*	PDI	2.70	1.81	1.77
	M_w (Da)	95×10^3	90×10^3	86×10^3

3.3 Scenario 2 evaluation

Figure 4 (a) shows the conversion evolution for the three simulated cases in scenario 2. In all cases, conversions below 65% were achieved at the end of the reaction time, a low value for styrene polymerization reactions. More linear conversion behavior was already expected because adding a continuous dosage of initiator controls the conversion rate. As expected, higher primer dosage rates led to higher conversions [41]. The simulation with the lowest BPO dosage rate (0.1 mol·min^{-1}) achieved a final conversion 55% less than the conversion achieved in the standard validation simulation. For the reaction with the highest BPO dosage rate (0.4 mol·min^{-1}), the value was 31% lower compared to the same case. Therefore, considering only the conversion efficiency, none of the cases led to process improvements. As can be seen in Figure 4 (b) – despite the high temperature and the possible inconveniences generated by the addition of the initiator only once – the initiator concentration at the beginning did not provide enough free radicals to obtain conversions of the same order as those achieved in the batch simulation. Figure 4 (c) shows the weight-average molar mass curves as a function of the conversion for the three cases in scenario 2. The reduction in the weight-average molar mass in the course of the reaction was already expected in all cases since the increase in the initiator concentration favors the formation of reduced molar mass polymers [42]. The case with the lowest BPO dosage rate had a weight-average final molar mass 50% higher compared to the highest dosage rate, i.e., the higher the dosage rate, the lower the weight-average molar mass,

as higher initiator concentration favors the termination reactions generating smaller polymer chains. Figure 4 (d) allows the corroboration of defined higher rates of initiator dosage lead to lower weight-average molar masses. The graphical analysis with the PDI and M_w values shown in Table 5 indicate that – in comparison with the standard – the initiator dosage also influences the characteristics of the final product leading to the production of a more homogeneous polymer with lower molar mass. As previously observed in scenario 1 with the heating ramp, the initiator dosage can also be applied to control the characteristics of polystyrene. However, the effect on the conversion rate must be considered since the conversion values obtained are not acceptable for industrial applications.

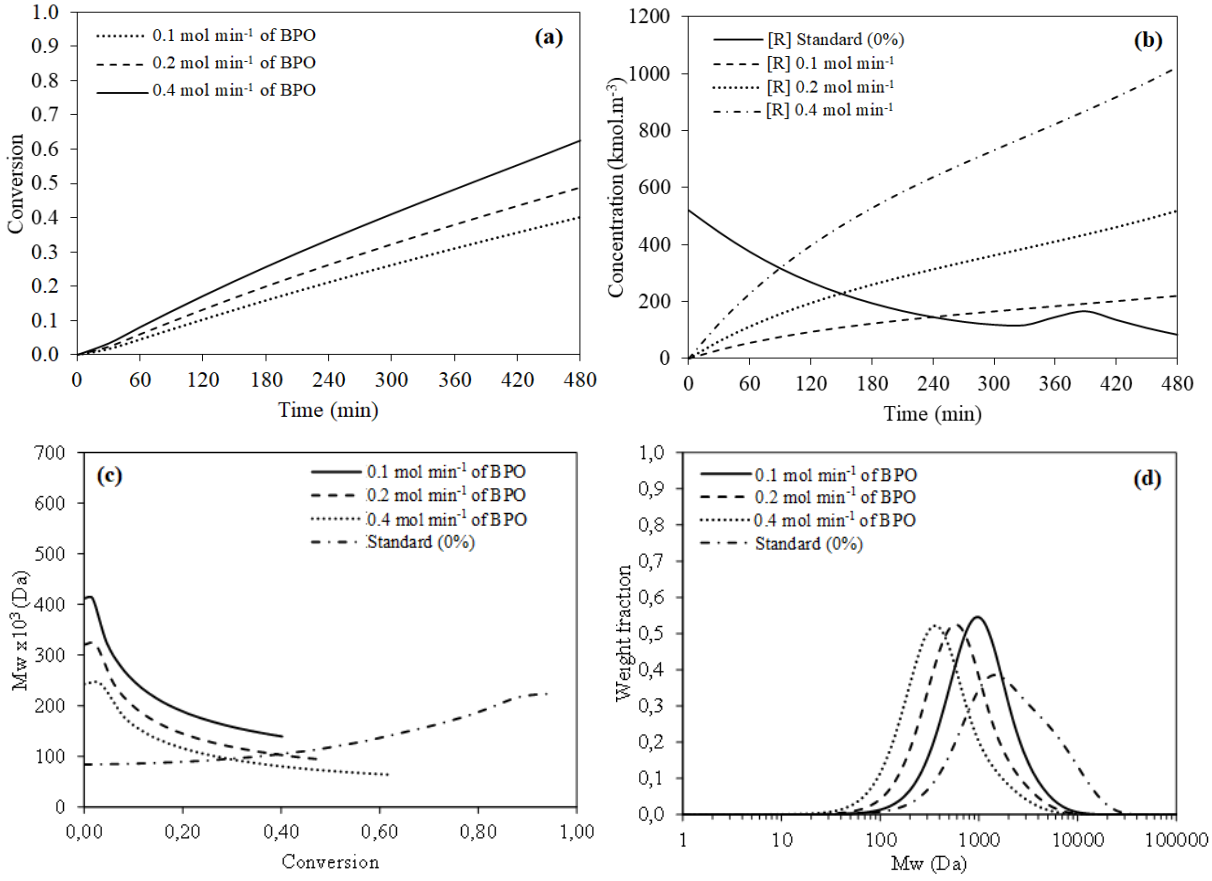


Fig. 4 Scenario 2: (a) conversion profile in relation to reaction time; (b) free radical concentration profiles. (c) evolution of Mw as a function of the conversion; (d) molar mass distribution at the end of the reaction.

Table 5 Polydispersity index (PDI) for reactions conducted in scenario 2

	0.1 mol·min^{-1}	**0.2 mol·min^{-1}**	**0.4 mol·min^{-1}**
PDI	1.92	2.05	2.17
M_w (Da)	140×10^3	94×10^3	58×10^3

3.4 Scenario 3 evaluation

Figure 5 (a) shows the conversion profile over time for scenario 3. Contrary to what was observed when all *n*-P_5 is added at the beginning of the reaction, in scenario 3, *n*-P_5 does not affect the initial reaction rate. Also, it has not a strong effect on the overall conversion rate, reaching over 95%. This can be explained by the low concentration of *n*-P_5 at the beginning of the reaction, which guarantees less dilution, not reducing the monomer and initiator concentrations, which were 10% higher at the beginning of the reaction. Figure 5 (b) shows the concentration profiles of the monomer, initiator, and blowing agent. At the end of the reaction, the *n*-P_5 content was reached, and the dosage rate was sufficient to inhibit the gel and glassy effects. In Figure 5 (c), similar behavior is shown between the simulation of scenario 3 (continuous dosage over reaction) and the case with dosing 7.5% of *n*-P_5 at the beginning of the reaction. However, in the case of continuous *n*-P_5 dosing, the reaction extent is about 30% higher, and the final weight-average molar mass is more than twice higher. Figure 5 (d) shows a shift and widening of the molar mass distribution towards the highest molar masses, corroborating the previous statement regarding the reaction extent. The curve widening also indicates that the EPS resulting from this reaction is more dispersed concerning the standard condition polymer, confirmed by the PDI (3.43). The highest molar mass reached (269×10^3 Da) confirms EPS production with higher mechanical resistance [43]. The global analysis of scenario 3 indicates that continuous *n*-P_5 dosing is advantageous. A higher conversion rate was achieved, and the blowing agent was dosed over the reaction, ruling out the need for another period of *n*-P_5 addition at the end of the reaction.

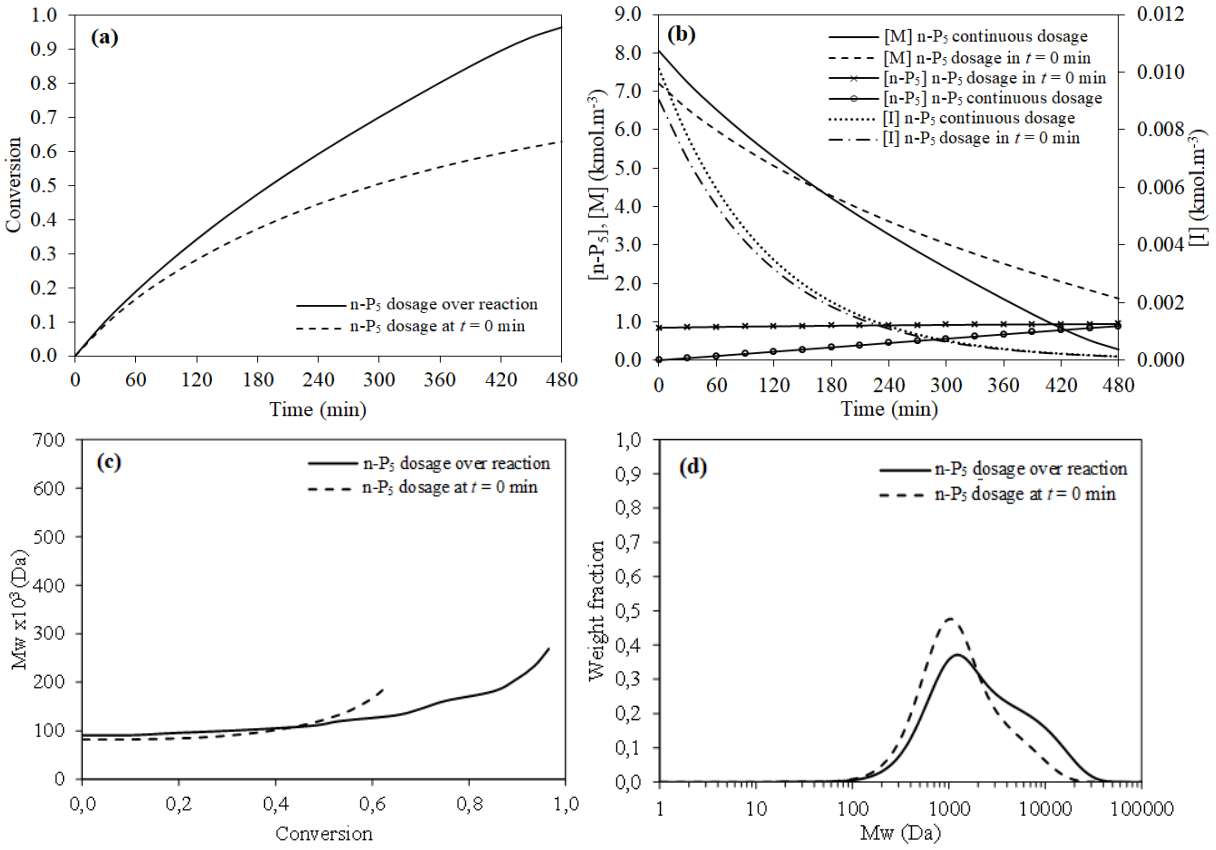


Fig. 5 Scenario 3: (a) conversion profile; (b) concentration profiles of monomer, initiator, and *n*-P5 of reactions; (c) evolution of weight-average molar mass as a function of the conversion; (d) molar mass distribution at the end of the reaction.

3.5 Scenario 4 evaluation

Scenario 4 is an extension of scenario 3, with the difference of investigating the action of a temperature ramp of 0.5 °C·min^{-1} (from 360 min to 420 min of reaction) and the dosage of BPO at a rate of 0.1 mol·min^{-1} in the same interval. Figure 6 shows the comparison between the scenarios 3 and 4. The heating ramp associated with the dosage of more initiator at the end of the reaction increases the conversion rate, as can be seen in Figure 6 (a), reaching 100%. The heating ramp and late initiator dosage circumvented the low conversion problems observed in scenarios 1 and 2 when these manipulations were performed at the beginning of the reaction. In this scenario, the heating ramp and intermediate addition of initiator were carried out at

360 min, when the conversion was already above 70% (above the PIP), which confers less risk of losing reaction stability [44]. Furthermore, as the addition of *n*-P_5 still occurred during the dosage of the initiator, its migration into the particles was guaranteed since *n*-P_5 is a solvent for PS. The heating rate of 0.5 °C·min^{-1} was chosen to reach 120 °C because the reaction rates increase with temperature. Moreover, at the temperature of 120 °C, the thermal initiation already has considerable influence [25], and adding more initiators guarantees the total consumption of the monomer. The average molar masses along the reaction are shown in Figure 6 (b). Different behavior was observed for the cases studied, mainly after 50% conversion, which shows the influence of the implemented changes on the properties of the produced polymers. The temperature rise in the last periods of reaction leads to an increase in reaction rates as there is an increase in the movement of macromolecules. This fact added to the contribution of thermal initiation, more the addition of an intermediate initiator favor termination reactions. It resulted in the profile of scenario 3 observed in Figure 6 (b), different from the accentuation of the curve of scenario 3. Figure 6 (c) shows that the monotonous profile observed in Figure 6 (b) is consistent with the narrower distribution in scenario 4, indicating the more homogeneous EPS production (PDI = 2.02) and lower weight-average molar mass (168×10^3 Da) concerning scenario 3. Therefore, manipulating process variables – late heating ramp, blowing agent dosage, and intermediate initiator dosage – proved to be an effective strategy for controlling the polymerization reaction and the properties of the synthesized EPS. Therefore, scenario 4 is an improved and promising EPS production pathway for potential industrial scale-up. Furthermore, the modifications by user-model routines in the commercial simulator mathematical model proved to be feasible to reliably describe the incorporating process of an expanding agent in the EPS synthesis, which allowed batch cycle improvements and resource savings.

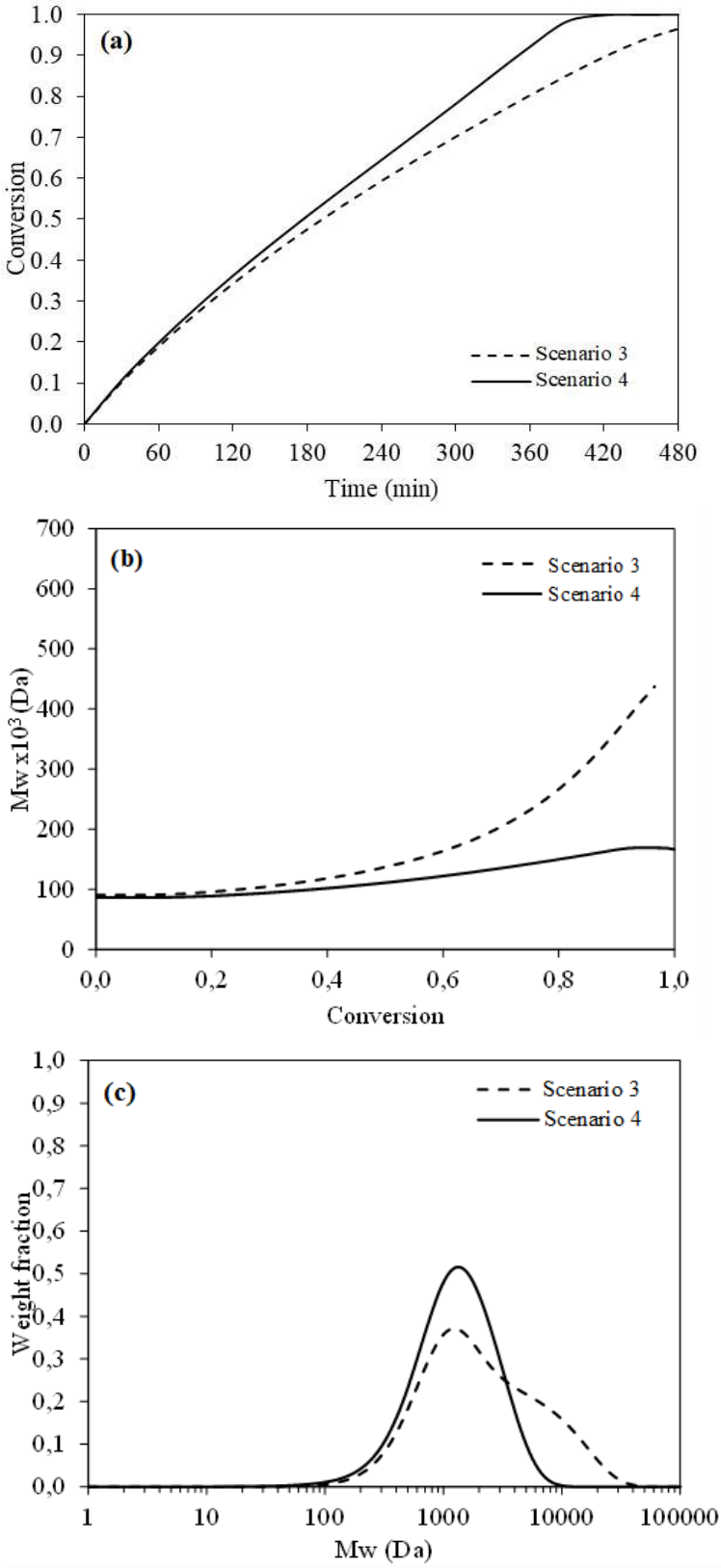


Fig. 6 Scenario 4 in comparison with scenario 3: (a) conversion profile in relation to reaction time; (b) evolution of M_w as a function of the conversion; (c) molar mass distribution at the end of the reaction.

4 Conclusion

Very long batch cycles are required to complete the polymerization and impregnation of EPS. It is known that the blowing agent, usually *n*-pentane, rubberizes the polymer matrix and influences the rate of polymerization and the average molar mass. One of the needs is to optimize the time for adding the blowing agent and the proportion of the initiator needed to improve productivity. However, the experimental evaluation of such parameters is expensive. In this work, the Aspen Polymers process simulator was used to evaluate different operational conditions for the production and impregnation of EPS. Changes were made to the standard mathematical model of the software through user-model routines that allow the study of specific cases, as the incorporation of gel and glass effects of adding the blowing agent in the simulations. The modified model was validated by reproducing experimental data from the literature. The influence of the implementation of heating ramps and the presence of different levels of expanding agent on the reaction kinetics and the average weight molar mass through different routes of EPS synthesis were studied. The conversion as a function of time, the weight-average molar mass as a function of the conversion, and the distribution curves of molar masses at the end of the reaction demonstrated that the process gains are possible only with the manipulation of operational conditions. Scenario 4, which only considers the temperature ramp and the addition of initiator at the end of the polymerization reaction, could be easily implemented on an industrial scale through conventional temperature and dosage control systems, respectively. Compared to all scenarios evaluated, scenario 4 led to maximum conversion in less time, which is extremely advantageous in industrial processes as it reduces the cycle of each batch. Therefore, the implemented changes proved to be effective in improving the dynamics of the EPS synthesis process.

Nomenclature

A	Adjustable parameter (-)
B	Adjustable parameter (-)
D_n	Dead polymer concentration ($\mathrm{mol\,L^{-1}}$)
f	Initiator efficiency (%)
I	Initiator concentration ($\mathrm{mol\,L^{-1}}$)
k_d	Decomposition kinetic constant ($\mathrm{h^{-1}}$)
k_i	Initiation kinetic constant ($\mathrm{h^{-1}}$)
k_p	Propagation kinetic constant ($\mathrm{h^{-1}}$)
k_{tc}	Combination termination kinetic constant ($\mathrm{h^{-1}}$)
k_{tf}	Chain transfer kinetic constant ($\mathrm{h^{-1}}$)
M	Monomer concentration ($\mathrm{mol\,L^{-1}}$)
M_0	Initial monomer concentration ($\mathrm{mol\,L^{-1}}$)
MM_m	Molar mass of the monomer ($\mathrm{g\,mol^{-1}}$)
M_n	Numerical mean molar mass ($\mathrm{g\,mol^{-1}}$)
M_w	Weight-average molar mass ($\mathrm{g\,mol^{-1}}$)
M_{wcr}	Critical mean mass molar mass ($\mathrm{g\,mol^{-1}}$)
n	Number of data points (-)
P_n	Concentration of live polymer ($\mathrm{mol\,L^{-1}}$)
R	Universal gas constant ($\mathrm{J\,mol^{-1}\,K^{-1}}$)
T	Temperature (K)
t	Time (s)
T_g	Glass transition temperature (K)

V Volume (m^3)

V_0 Initial volume (m^3)

VF Free volume (m^3)

VF_{cr} Critical free volume (m^3)

V_m Monomer volume (m^3)

V_p Polymer volume (m^3)

V_s Solvent volume (m^3)

X Conversion (-)

X_s Conversion at the time of *n*-P5 feeding (-)

Y_i Experimental value (-)

$\hat{Y}_i$ Predicted value (-)

Greek letters

δ Jump distance (nm)

λ_k Moment for live polymer (mol m^{-3})

μ_k Moment for dead polymer (mol m^{-3})

Declarations

Availability of data and material The data supporting the findings of this study are available from the corresponding author upon reasonable request.

Funding This study was financed in part by the Coordenação de Aperfeiçoamento de Pessoal de Nível Superior – Brasil (CAPES) – Finance Code 001.

Competing interests The authors declare that they have no competing interests.

Authors' contributions JLSA: Investigation, Methodology, Software, Validation, Visualization, Formal analysis, and Writing – original draft. RB: Formal analysis, Writing – original draft, and Writing – review & editing. RAFM: Conceptualization, Methodology, Supervision, and Writing – review & editing. CM: Conceptualization, Methodology, Supervision, and Writing – review & editing. All authors read and approved the final manuscript.

Acknowledgements The authors acknowledge the Federal Institute of Education, Science and Technology of Santa Catarina (IFSC) and the Federal University of Santa Catarina (UFSC) for their institutional and technical support.

References

1. Cella RF, Mumbach GD, Andrade KL, et al (2018) Polystyrene recycling processes by dissolution in ethyl acetate. J Appl Polym Sci 135:46208. https://doi.org/10.1002/app.46208
2. Uttaravalli AN, Dinda S, Gidla BR (2020) Scientific and engineering aspects of potential applications of post-consumer (waste) expanded polystyrene: A review. Process Saf Environ Prot 137:140–148. https://doi.org/https://doi.org/10.1016/j.psep.2020.02.023
3. Chaudhary V, Sharma S (2019) Suspension polymerization technique: parameters affecting polymer properties and application in oxidation reactions. J Polym Res 26:102. https://doi.org/10.1007/s10965-019-1767-8
4. Raps D, Hossieny N, Park CB, Altstädt V (2015) Past and present developments in polymer bead foams and bead foaming technology. Polymer (Guildf) 56:5–19. https://doi.org/https://doi.org/10.1016/j.polymer.2014.10.078
5. Brooks B (2010) Suspension polymerization processes. Chem Eng Technol 33:1737–

1744. https://doi.org/10.1002/ceat.201000210

6. Horie K, Mita I, Kambe H (1968) Calorimetric investigation of polymerization reactions. I. Diffusion-controlled polymerization of methyl methacrylate and styrene. J Polym Sci Part A-1 Polym Chem 6:2663–2676. https://doi.org/10.1002/pol.1968.150060921
7. Hajova H, Chmelar J, Nistor A, et al (2013) Experimental Study of Sorption and Diffusion of n-Pentane in Polystyrene. J Chem Eng Data 58:851–865. https://doi.org/10.1021/je300916f
8. Mehravar E, Abbasi F, Jalili K, et al (2012) Synthesis and expansion characteristics of expandable styrene/methyl methacrylate copolymer beads: The effects of monomer composition and cell structure modifying aid. J Cell Plast 48:161–190. https://doi.org/10.1177/0021955X11433225
9. Machado RAF, Pinto JC, Araújo PHH, Bolzan A (2000) Mathematical modeling of polystyrene particle size distribution produced by suspension polymerization. Brazilian J Chem Eng 17:395–407. https://doi.org/10.1590/S0104-66322000000400004
10. Curteanu S (2003) Modeling and simulation of free radical polymerization of styrene under semibatch reactor conditions. Cent Eur J Chem 1:69–90. https://doi.org/10.2478/BF02479259
11. Almeida AS, Wada K, Secchi AR (2008) Simulation of styrene polymerization reactors: kinetic and thermodynamic modeling. Brazilian J Chem Eng 25:337–349. https://doi.org/10.1590/S0104-66322008000200012
12. Srivastava A, Ghosh S (2010) Evaluating the Glass Transition Temperature of Polystyrene by an Experimentally Validated Molecular Dynamics Model. Int J Multiscale Comput Eng 8:. https://doi.org/10.1615/IntJMultCompEng.v8.i5.80
13. Vieira RP, Lona LMF (2016) Simulation of temperature effect on the structure control of polystyrene obtained by atom-transfer radical polymerization. Polímeros 26:313–

319. https://doi.org/10.1590/0104-1428.2376

14. Khajehpour-Tadavani S, Abedini H, Nekoomanesh-Haghighi M (2025) Simulation of particle size distribution of polystyrene/expandable polystyrene in suspension polymerization with the use of modified time increment Monte Carlo model. J Polym Res 32:333. https://doi.org/10.1007/s10965-025-04536-4
15. Makwana Y, Moudgalya KM, Khakhar D V. (1997) Modeling of industrial styrene polymerization reactors. Polym Eng Sci 37:1073–1081. https://doi.org/10.1002/pen.11752
16. Lobry E, Lasuye T, Gourdon C, Xuereb C (2015) Liquid–liquid dispersion in a continuous oscillatory baffled reactor – Application to suspension polymerization. Chem Eng J 259:505–518. https://doi.org/10.1016/j.cej.2014.08.014
17. Salejova G, Kosek J (2006) Dynamics of foaming of polystyrene particles. Macromol Symp 243:233–246. https://doi.org/10.1002/masy.200651122
18. Victoria-Valenzuela D, Morales-Cepeda AB (2022) Contributing to a better comprehension of: the styrene bulk free-radical polymerization with n-pentane added as a blowing agent for producing expandable polystyrene. J Polym Res 29:392. https://doi.org/10.1007/s10965-022-03201-4
19. Lesage F, Nedelec D, Descales B, Stephens WD (2012) Dynamic Modelling of a Polypropylene Production Plant. In: Bogle IDL, Fairweather M (eds) 22nd European Symposium on Computer Aided Process Engineering. Elsevier, p 1128
20. Funai VI, Melo DNC, Lima NMN, et al (2014) Attainment of Kinetic Parameters and Model Validation for Nylon-6 Process. In: Klemeš JJ, Varbanov PS, Liew PY (eds) 24th European Symposium on Computer Aided Process Engineering. Elsevier, pp 1483–1488
21. Kusolsongtawee T, Bumroongsri P (2017) Optimization of Energy Consumption in Gas-Phase Polymerization Process for Linear Low Density Polyethylene Production.

Energy Procedia 138:772–777. https://doi.org/10.1016/j.egypro.2017.10.055

22. Scorah MJ, Dhib R, Penlidis A (2006) Modelling of free radical polymerization of styrene and methyl methacrylate by a tetrafunctional initiator. Chem Eng Sci 61:4827–4859. https://doi.org/10.1016/j.ces.2006.03.018

23. Bishop RB (1971) Practical polymerization for polystyrene. Cahners Publishing Co., Massachusetts

24. Villalobos MA, Hamielec AE, Wood PE (1993) Bulk and suspension polymerization of styrene in the presence of n-pentane. An evaluation of monofunctional and bifunctional initiation. J Appl Polym Sci 50:327–343. https://doi.org/10.1002/app.1993.070500214

25. Hui AW, Hamielec AE (1972) Thermal polymerization of styrene at high conversions and temperatures. An experimental study. J Appl Polym Sci 16:749–769. https://doi.org/10.1002/app.1972.070160319

26. D'hooge DR, Reyniers M-F, Marin GB (2009) Methodology for Kinetic Modeling of Atom Transfer Radical Polymerization. Macromol React Eng 3:185–209. https://doi.org/10.1002/mren.200800051

27. Machado F, Lima EL, Pinto JC (2007) Uma revisão sobre os processos de polimerização em suspensão. Polímeros 17:166–179. https://doi.org/10.1590/S0104-14282007000200016

28. Elbro HS, Fredenslund A, Rasmussen P (1991) Group contribution method for the prediction of liquid densities as a function of temperature for solvents, oligomers, and polymers. Ind Eng Chem Res 30:2576–2582. https://doi.org/10.1021/ie00060a011

29. Villalobos MA, Hamielec AE, Wood PE (1991) Kinetic model for short-cycle bulk styrene polymerization through bifunctional initiators. J Appl Polym Sci 42:629–641. https://doi.org/10.1002/app.1991.070420309

30. Choi KY, Liang WR, Lei GD (1988) Kinetics of bulk styrene polymerization catalyzed by symmetrical bifunctional initiators. J Appl Polym Sci 35:1547–1562.

https://doi.org/10.1002/app.1988.070350612

31. Mahabadi HK, O'Driscoll KF (1977) Concentration Dependence of the Termination Rate Constant During the Initial Stages of Free Radical Polymerization. Macromolecules 10:55–58. https://doi.org/10.1021/ma60055a009

32. Battisti R, Claumann CA, Manenti F, et al (2020) Dynamic modeling with experimental validation and control of a two-phase closed thermosyphon as heat supplier of a novel pilot-scale falling film distillation unit. Comput Chem Eng 143:107078. https://doi.org/10.1016/j.compchemeng.2020.107078

33. Maul J, Frushour BG, Kontoff JR, et al (2000) Polystyrene and Styrene Copolymers. In: Ullmann's Encyclopedia of Industrial Chemistry. American Cancer Society

34. Crevecoeur JJ, Nelissen L, Lemstra PJ (1999) Water expandable polystyrene (WEPS): Part 1. Strategy and procedures. Polymer (Guildf) 40:3685–3689. https://doi.org/10.1016/S0032-3861(98)00617-X

35. Fen-Chong T, Hervé É, Dubault A, Halary JL (1999) Viscoelastic Characteristics of Pentane-Swollen. J Appl Polym Sci 73:2463–2472. https://doi.org/10.1002/(SICI)1097-4628(19990919)73:12<2463::AID-APP15>3.0.CO;2-U

36. Achilias DS (2007) A Review of Modeling of Diffusion Controlled Polymerization Reactions. Macromol Theory Simulations 16:319–347. https://doi.org/10.1002/mats.200700003

37. Tefera N, Weickert G, Westerterp KR (1997) Modeling of free radical polymerization up to high conversion. I. A method for the selection of models by simultaneous parameter estimation. J Appl Polym Sci 63:1649–1661. https://doi.org/10.1002/(SICI)1097-4628(19970321)63:12<1649::AID-APP16>3.0.CO;2-V

38. Çetinkaya S, Zeybek Z, Hapoğlu H, Alpbaz M (2006) Optimal temperature control in a

batch polymerization reactor using fuzzy-relational models-dynamics matrix control. Comput Chem Eng 30:1315–1323. https://doi.org/10.1016/j.compchemeng.2006.04.002

39. Odian G (2004) Radical Chain Polymerization. In: Principles of Polymerization, 4 ed. pp 198–349

40. Santos JC, Reis MM, Machado RAF, et al (2004) Online Monitoring of Suspension Polymerization Reactions Using Raman Spectroscopy. Ind Eng Chem Res 43:7282–7289. https://doi.org/10.1021/ie034278m

41. Kiparissides C, Macgregor JF, Hamielec AE (1980) Continuous emulsion polymerization of vinyl acetate. Part I: Experimental studies. Can J Chem Eng 58:48–55. https://doi.org/10.1002/cjce.5450580108

42. Ding J, Yang C, Zhou L, et al (2025) Free Radical Polymerization of Styrene and Maleimide Derivatives: Molecular Weight Control and Application as a Heat Resistance Agent. Molecules 30:. https://doi.org/10.3390/molecules30091863

43. Martin JR, Johnson JF, Cooper AR (1972) Mechanical Properties of Polymers: The Influence of Molecular Weight and Molecular Weight Distribution. J Macromol Sci Part C 8:57–199. https://doi.org/10.1080/15321797208068169

44. Gonçalves OH, Nogueira AL, Araújo PHH, Machado RAF (2011) Effects of Operational Parameters on Particle Size Distributions in Methyl Methacrylate Suspension Polymerization. Ind Eng Chem Res 50:9116–9122. https://doi.org/10.1021/ie200230j